Linearized extended waveform inversion via Differential Semblance Optimization in the Depth-oriented Extension

Yujin Liu[*†], *William W. Symes*[†], *Yin Huang*[†],*and Zhenchun Li*[*], [*]*China University of Petroleum (Huadong),*[†]*Rice University*

SUMMARY

Waveform inversion is prone to local minimum when there is no low frequency or long offset information in seismic reflection data. One effective way to solve this problem is extending model space and introducing extended modeling. However, if we extend model space in depth-oriented domain, which is free of kinematic artifacts, the computational cost of corresponding extended modeling is extremely high. Based on linearized Born approximation, we split the model into two components (i.e. long scales and short scales) and only extend short scales, then the previous extended waveform inversion problem can be solved by two-stage scheme, the first stage is to solve a linear inverse problem with respect to short scales, the second stage is to solve a nonlinear inverse problem with respect to long scales. Differential semblance term is incorporated into the objective function to solve the problem of local minimum in the second stage. With this hybrid two-term objective function, we can derive the gradient formulas for short scales and long scales respectively. During the derivation, Chebyshev iteration, rather than conjugate gradient method is justified in solving the linear inverse problem. Even though only subsurface offset extension in the acoustic constant density medium is discussed in this abstract, most of the formulas and algorithms can be extended into other model extensions and more complex medium. Numerical tests on Gaussian anomaly model demonstrates the effectiveness of our proposed method.

INTRODUCTION

Seismic velocity analysis methods can be divided into two groups. The first group aims at minimizing the misfit in the data domain, such as waveform inversion (WI) (Tarantola, 1984; Pratt, 1999; Virieux and Operto, 2009), while the second group aims at improving the quality in the image domain, such as migration velocity analysis (MVA) (Symes and Carazzone, 1991; Biondi and Sava, 1999; Shen and Symes, 2008). The data domain methods take into account essentially any physics of seismic wave propagation that can be modeled, they have the advantage of high resolution in the inverted model, but the waveform inversion objective has many spurious local minimum when seismic data lacks low frequencies or initial model is not accurate enough. The image domain methods, on the other hand, have the advantage of quasi-global convergence if we choose objective appropriately. However, as only transmission information is used in the image domain method, the vertical resolution of inverted velocity model is limited.

One natural way to solve above problems is to invert background velocity with MVA firstly and then use it as initial model for WI, but in practice, it's very hard to determine whether the initial model derived from MVA is accurate enough for WI. In fact, It has been demonstrated that MVA is the partially linearized version of waveform inversion, it can be linked with WI under the concept of extended modeling (Symes, 2008), which provides a big opportunity to combine them together and invert all the wavelengths of the model simultaneously (Sun and Symes, 2012; Biondi and Almomin, 2012; Almomin and Biondi, 2012).

With the concept of depth-oriented model extension, the scaler of velocity in conventional seismic modeling becomes an operator in extended modeling (Symes, 2008; Biondi and Almomin, 2012), which makes extended waveform inversion extremely expensive and impractical at present. In this abstract, we split the extended model into two components, i.e. short scales and long scales, and extend only short scales. Based on linearized Born approximation, we derive the gradient for short scales and long scales of model from the objective function which combines data misfitting and differential semblance term. As short scales of model are also inverted with Chebyshev iterations, rather than prestack migration approximation, in the inner loop of background velocity update, the new scheme is more accurate from the origin. Numerical tests demonstrates the effectiveness of our proposed method.

THEORY

Extended waveform inversion

The premise of WI is that there exists a forward map or prediction operator F, which relates the model space M (a set of possible models of Earth structure) to the data space D (a set of seismic data). While WI finds $m \in M$ to minimize the mean square data misfit between the forward map output $F[m]$ and an observed data $d \in D$, that is:

$$min_m J_{WI}[m,d] = \frac{1}{2} \parallel F[m] - d \parallel^2 \qquad (1)$$

in which the symbol $\parallel \cdot \parallel^2$ stands for ℓ_2 norm.

In order to establish the relation between WI and MVA, The concept of extended modeling $\bar{F}$, which maps the extended model space $\bar{M}$ to data space D, was introduced (Symes, 2008). Extension operator, which maps model space from M to $\bar{M}$, has two main properties, that is, (1) $M \subset \bar{M}$ (2) $\bar{F}[\bar{m}] = F[m]$, if $m \in M$. Accordingly, extended waveform inversion finds $\bar{m} \in \bar{M}$ to minimize the mean square data misfit between the extended modeling output $\bar{F}[\bar{m}]$ and an observed data $d \in D$, that is:

$$min_{\bar{m}} J_{EWI}[\bar{m},d] = \frac{1}{2} \parallel \bar{F}[\bar{m}] - d \parallel^2 \qquad (2)$$

However, if we solve above problem directly, the ambiguity of solutions is more likely to happen due to the fact that the

extended model space has more degree of freedom, so we need to restrict the solution to be the physical one, then the inverse problem becomes to finding the physical one in the feasible model set constrained by the data fitting, that is,

$$min_{\bar{m}}J_{DS}[\bar{m},d] = \frac{1}{2}\parallel A[\bar{m}]\parallel^2, s.t.: \frac{1}{2}\parallel \bar{F}[\bar{m}]-d\parallel^2\leq \varepsilon \quad (3)$$

which is equivalent to the following unconstrained inverse problem under some conditions:

$$min_{\bar{m}}\tilde{J}_{EWI}[\bar{m},d] = \sigma\parallel A[\bar{m}]\parallel^2 + \parallel \bar{F}[\bar{m}]-d\parallel^2 \quad (4)$$

where A is an annihilator which maps extended model space $\bar{M}$ to some other Hilbert space. It depends on the types of model extension: (1) When extension is along subsurface space shift domain, $A[\bar{m}]$ is a diagonal matrix with offset as the diagonal elements; (2) When extension is along time axis, $A[\bar{m}]$ is a annihilator to suppress non-zero time lag; (3) When extension is along surface axis, such as source index, source-receiver offset, plane-wave slope, $A[\bar{m}]$ is one-order derivative operator to impose coherence. In this paper, we focus on depth-oriented offset extension. where σ is the penalty parameter, when $\sigma = 0$, Equation 4 limits to the problem of extended waveform inversion, when $\sigma \rightarrow \infty$, Equation 4 limits to the problem of non-linear MVA.

Linearized extended waveform inversion

Split extended model $\bar{m} \in \bar{M}$ into two parts, the first one is long scales $m_0 \in M$, the second one is short scales $\delta\bar{m} \in \bar{M}$, that is,

$$\bar{m} \simeq m_0 + \delta\bar{m} \quad (5)$$

If m_0 is smooth and $\delta\bar{m}$ is rough or oscillatory on the wavelength scale (well-separated scales), then extended forward modeling operator $\bar{F}[\bar{m}]$ can be approximated with small error as follows (Symes, 2009):

$$\bar{F}[\bar{m}] \simeq F[m_0] + DF[m_0] * \delta\bar{m} \quad (6)$$

where $DF[m_0]$ is one order derivative of F to m at m_0, which is also called linearized Born operator in geophysics, Then the inverse problem becomes to:

$$min_{m_0,\delta\bar{m}}J_{DS}[m_0,\delta\bar{m}] =\parallel DF[m_0]\delta\bar{m}-F_d\parallel^2 +\sigma\parallel A\delta\bar{m}\parallel^2 \quad (7)$$

Where $F_d = d - F[m_0]$ is the observed seismic data after subtracting the modeled data with initial model. In practice, the first term is often approximated by the result of adjoint of Born operator (migration operator) applied to seismic data and then solve the second term with the method namely called migration velocity analysis.

In this paper, we also adopt this two-stage scheme, but with more precise derivation and calculations. Correspondingly, the first stage is to solve problem 7 with respected to $\delta\bar{m}$, which is a quadratic inverse problem and can be solved stably with gradient methods, while the second stage is to solve problem 7 respected to m_0, which is a nonlinear and often non-convex inverse problems. However, there are some numerical and theoretical results show that the second problem is quasi-convex if we choose A as differential semblance operator.

The key to solve these two inverse problems is calculating their gradients. Firstly, Let's look at the gradient of the objective function $J_{DS}[m_0,\delta\bar{m}]$ with respect to $\delta\bar{m}$. The gradient can be derived easily as follows:

$$\nabla_{\delta\bar{m}}J_{DS}[m_0,\delta\bar{m}] = DF^T[m_0](DF[m_0]\delta\bar{m} - F_d)+\sigma A^T A\delta\bar{m} \quad (8)$$

Set the gradient to zero gives the normal equation, i.e.

$$(DF^T[m_0]DF[m_0] + \sigma A^T A)\delta\bar{m} = DF^T[m_0]F_d \quad (9)$$

which can be re-written as:

$$N[m_0]\delta\bar{m} = M[m_0]F_d \quad (10)$$

where $N[m_0]$ is normal operator and $M[m_0]$ is migration operator.

After minimizing the objective function $J_{DS}[m_0,\delta\bar{m}]$ with respect to $\delta\bar{m}$, we can start the second stage, which minimizes the objective function $J_{DS}[m_0,\delta\bar{m}[m_0]]$ with respect to m_0. Let's calculate the directional derivative of J_{DS} in the direction of m_0,

$$D_{m_0}J_{DS}[m_0,\delta\bar{m}[m_0]]dm_0 = D_{m_0}J_{DS}[m_0,\delta\bar{m}[m_0]]dm_0+$$
$$(D_{\delta\bar{m}}J_{DS}[m_0,\delta\bar{m}[m_0]])^T D_{m_0}\delta\bar{m}dm_0 \quad (11)$$

If we first assume that we have solved the first problem accurately, the second term in equation 11 will be vanished. Since the differential semblance term is independent of m_0, we can obtain:

$$D_{m_0}J_{DS}[m_0,\delta\bar{m}[m_0]]dm_0$$
$$= \langle D(DF[m_0]\delta\bar{m})dm_0, DF[m_0]\delta\bar{m} - F_d\rangle$$
$$= \langle dm_0, B[\delta\bar{m},DF[m_0]\delta\bar{m} - F_d]\rangle \quad (12)$$

where B is bilinear operator. In fact, the second term in 11 can be very large, even when the normal equation is solved rather precisely, because it involves the derivative of the reflectivity estimate with respect to velocity. It is the anomalously large size of the derivative of the synthetic data with respect to velocity that led to non-convexity of the mean-square error function. For exactly the same reason (phase perturbation of rapidly oscillating signals), neglect of the second term in equation 8 will leads to large errors (Symes and Kern, 1994).

Any iterative scheme for $\delta\bar{m}$ of equation 10 gives the following approximation:

$$\delta\bar{m} = P(N[m_0])M[m_0]F_d \quad (13)$$

where $P(N[m_0])$ is a polynomial in the normal operator $N[m_0]$. Take the derivative of $\delta\bar{m}$ with respect to m_0, we can get:

$$D_{m_0}\delta\bar{m}dm_0$$
$$= \sigma(D_N P(N[m_0])DN[m_0]dm_0 M[m_0]F_d + P(N[m_0])D(M[m_0]F_d)dm_0) \quad (14)$$

In the case of depth-oriented model extension, normal operator will not change the phase of input, while migration operator will dramatically change the phase of input when background model is changed (Stolk et al., 2009), so $DN[m_0]dm_0$

is relatively very small compared with $DM[m_0]dm_0$. Moreover, $D_N P(N[m_0])$ is bounded if we use Chebyshev iteration, which it's not the case if we use CG method, *So we can drop the first term of equation 14 if we use Chebyshev iteration to solve equation 10 in the case of depth-oriented model extension*. Then equation 14 changes to:

$$D_{m_0}\delta\bar{m}dm_0 = P(N[m_0])D(M[m_0]F_d)dm_0$$
$$= P(N[m_0])D(DF^T[m_0]F_d)dm_0 \quad (15)$$

After k iterations at the first stage of reflectivity inversion, $D_{\delta\bar{m}}J_{DS}[m_0,\delta\bar{m}]$, the normal equation error, can be denoted as e_k, and $\delta\bar{m}$ by $\delta\bar{m}_k$. Then equation 11 becomes:

$$D_{m_0}J_{DS}[m_0,\delta\bar{m}[m_0]]dm_0$$
$$= \langle dm_0, B[\delta\bar{m}_k, DF[m_0]\delta\bar{m}_k - F_d]\rangle +$$
$$\langle e_k, P(N[m_0])D(DF^T[m_0]F_d)dm_0\rangle$$
$$= \langle dm_0, B[\delta\bar{m}_k, DF[m_0]\delta\bar{m}_k - F_d]\rangle +$$
$$\langle dm_0, B[P(N[m_0])e_k, F_d]\rangle \quad (16)$$

At last, we can get the gradient formula as follows,

$$\nabla_{m_0}J_{DS}[m_0,\delta\bar{m}[m_0]]$$
$$= B[\delta\bar{m}_k, DF[m_0]\delta\bar{m}_k - F_d] + B[P(N[m_0])e_k, F_d] \quad (17)$$

Acoustic constant density medium case

We should claim firstly that even though the following derivation is done in frequency domain, the actual implementation is done in time domain. In the acoustic constant density medium, wave propagation can be formulated in the frequency domain as:

$$(\nabla^2 + \omega^2 m(\mathbf{x},z))u(\mathbf{x},z,\omega) = f(\omega)\delta(\mathbf{x}-\mathbf{x}_s) \quad (18)$$

where $\mathbf{x}$ is the horizontal vector, z is the depth axis, $\mathbf{x}_s$ is the source position, $m(\mathbf{x},z)$ is squared slowness, $u(\mathbf{x},z,\omega)$ is the seismic wavefield at frequency ω, $f(\omega)$ is the spectrum of source function. We should note that $m(\mathbf{x},z)$ is a scaler here.

Based on the idea of extended modeling, equation 18 changes to:

$$\nabla^2 u(\mathbf{x},z,\omega) + \omega^2 \int d\mathbf{y} m(\mathbf{x},\mathbf{y},z)u(\mathbf{y},z,\omega) = f(\omega)\delta(\mathbf{x}-\mathbf{x}_s) \quad (19)$$

where $m(\mathbf{x},\mathbf{y},z)$ becomes to be an operator. When $m(\mathbf{x},z) = m(\mathbf{x},\mathbf{y},z)\delta(\mathbf{x}-\mathbf{y})$, equation 19 is equivalent to equation 18.

Split the extended model into two parts as follows:

$$m(\mathbf{x},\mathbf{y},z) = b(\mathbf{x},z)\delta(\mathbf{x}-\mathbf{y}) + r(\mathbf{x},\mathbf{y},z) \quad (20)$$

where $b(\mathbf{x},z)$ is background velocity and $r(\mathbf{x},\mathbf{y},z)$ is extended reflectivity. Correspondingly, split the wavefield into two parts, i.e. $u(\mathbf{x},\mathbf{y},z,t) = u_0(\mathbf{x},\mathbf{y},z,t) + \delta u(\mathbf{x},\mathbf{y},z,\omega)$, then after linearized approximation, equation 18 changes to:

$$(\nabla^2 + \omega^2 b(\mathbf{x},z))\delta u(\mathbf{x},z,\omega) = -\omega^2 \int d\mathbf{y} r(\mathbf{x},\mathbf{y},z)u_0(\mathbf{y},z,\omega) \quad (21)$$

where $u_0(\mathbf{y},z,\omega)$ satisfies:

$$(\nabla^2 + \omega^2 b(\mathbf{x},z))u_0(\mathbf{x},z,\omega) = f(\omega)\delta(\mathbf{x}-\mathbf{x}_s) \quad (22)$$

The solution of equation 22 can be written as:

$$u_0(\mathbf{x},z,\omega) = f(\omega)G(\mathbf{x},\mathbf{x}_s,\omega) \quad (23)$$

where $G(\mathbf{x},\mathbf{x}_s,\omega)$ is the Green function, which is the seismic wave responds after exciting a spike at position $\mathbf{x}_s$. Seismic data $d(\mathbf{x}_r,\mathbf{x}_s,\omega)$ can be approximated modeled by the solution $\delta u(\mathbf{x},z,\omega)$ of equation 21 at the predefined source locations $\mathbf{x}_s$ and receiver locations $\mathbf{x}_r$. Define $\mathbf{y} = \mathbf{x} + 2\mathbf{h}$, replace $\mathbf{x}$ with $\mathbf{x} - \mathbf{h}$ and assuming $z_s = z_r = 0$, The modeling formula can be expressed as:

$$d(\mathbf{x}_r,\mathbf{x}_s,\omega) =$$
$$-\omega^2 f(\omega) \int d\mathbf{x} d\mathbf{h}\, G(\mathbf{x}_r,\mathbf{x}+\mathbf{h},\omega)r(\mathbf{x},\mathbf{h})G(\mathbf{x}-\mathbf{h},\mathbf{x}_s,\omega) \quad (24)$$

From equation 24, we can see the linear relation between seismic data and model perturbation. This is actually the output of linearized Born modeling operator, i.e. $DF[b(\mathbf{x})]r(\mathbf{x},\mathbf{h})$. Adjoint of Born modeling is:

$$r(\mathbf{x},\mathbf{h}) =$$
$$-\int d\mathbf{x}_s d\mathbf{x}_r d\omega\, \omega^2 f^*(\omega)G^*(\mathbf{x}_s,\mathbf{x}-\mathbf{h},\omega)G^*(\mathbf{x}+\mathbf{h},\mathbf{x}_r,\omega)d(\mathbf{x}_r,\mathbf{x}_s,\omega) \quad (25)$$

This is actually the output of the adjoint of linearized Born operator with $d(\mathbf{x}_r,\mathbf{x}_s,\omega)$ as input, i.e. $DF^T[b(\mathbf{x})]d(\mathbf{x}_r,\mathbf{x}_s,\omega)$, which is often called space-shift imaging condition (Rickett and Sava, 2002; Biondi and Symes, 2004).

Similarly, we can get the bilinear operator with perturbation on background velocity. The final formula is:

$$\Delta b(\mathbf{y}) =$$
$$\int d\mathbf{x}_s d\mathbf{x}_r d\mathbf{x} d\mathbf{h} d\omega \left\{ G_0(\mathbf{y},\mathbf{x}_s,\omega)\omega^4 f(\omega) \right\}^*$$
$$\left\{ G_0^*(\mathbf{y},\mathbf{x}-\mathbf{h},\omega)r(\mathbf{x},\mathbf{h})G_0^*(\mathbf{x}+\mathbf{h},\mathbf{x}_r,\omega)\Delta d(\mathbf{x}_r,\mathbf{x}_s,\omega) \right\} +$$
$$\int d\mathbf{x}_s d\mathbf{x}_r d\mathbf{x} d\mathbf{h} d\omega \left\{ G_0(\mathbf{y},\mathbf{x}+\mathbf{h},\omega)r(\mathbf{x},\mathbf{h})G_0(\mathbf{x}-\mathbf{h},x_s,\omega)\omega^4 f(\omega) \right\}^*$$
$$\left\{ G_0^*(\mathbf{y},\mathbf{x}_r,\omega)\Delta d(\mathbf{x}_r,\mathbf{x}_s,\omega) \right\}. \quad (26)$$

which defines the output of bilinear operator with $r(\mathbf{x},\mathbf{h})$ and $\Delta d(\mathbf{x}_r,\mathbf{x}_s,\omega)$ as input, i.e. $B[r(\mathbf{x},\mathbf{h}),DF[b(\mathbf{x})]r(\mathbf{x},\mathbf{h}) - \Delta d(\mathbf{x}_r,\mathbf{x}_s,\omega)]$.

NUMERICAL TESTS

Gaussian model, which contains a Gaussian anomaly in the two-layer model, is used in the numerical tests. The velocity for the top layer, bottom layer and peak of the Gaussian anomaly are 3 km/s, 3.5 km/s and 3.5 km/s respectively. Figure 1(a) shows the true velocity model. A Ricker wavelet with a fundamental frequency of 15 Hz and temporal sampling of 0.75 ms is used as a source function to model the data. There are 151 fixed receivers with a spacing of 20 m and 31 sources with a spacing of 100 m. The maximum offset used is 1.5 km in both sides and the initial model is a constant model of 3 km/s velocity. Synthetic seismic data cube is shown in the figure 1(b). Constant velocity model with velocity of 3 km/s is used as the initial velocity model in our numerical test.
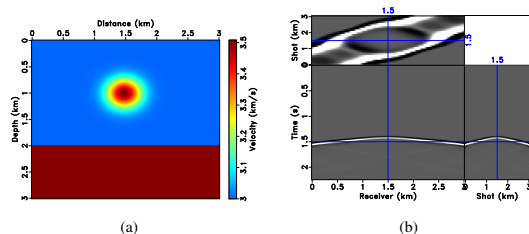
Figure 1: (a) Gaussian velocity model; (b) Synthetic data.

As we demonstrated in the theory section, in the inner loop of background velocity update, Chebyshev iteration, rather than conjugate gradient method, is used to solve the normal equation 10. Figure 2(a) shows the result of prestack reverse time migration, we can see that the layer is not flat and subsurface offset gather does not focus on zero offset due to the velocity error. Figure 2(b) shows the inverted reflectivity by Chebyshev iteration method. Compared with figure 2(a), we can see that the inverted result has higher resolution, more balanced amplitude and more focused energy near zero offset. With the inverted reflectivity, we can calculate the data misfit residual, which shows in figure 2(c). Figure 2(d) shows the relative normal residual of Chebyshev iteration, we can see that it can achieve a very small residual (0.043 at the last iteration) even though the spectrum bound was reseted several times at each jump on the curve.
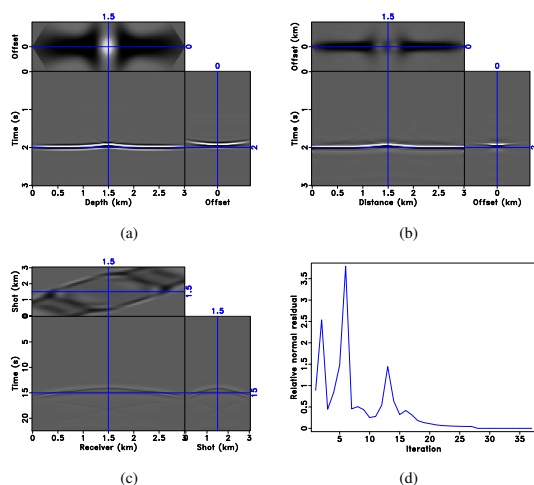

Figure 2: (a) Reflectivity with prestack reverse-time migration; (b) Inverted reflectivity with Chebyshev iteration method; (c) Data misfit residual of Chebyshev iteration method in the same scale with figure 1(b); (d) Relative normal residual curve.

Figure 3(a) shows the first term of gradient formula in equation 17, we can see that the negative gradient shows the update direction of background velocity correctly even though it contains very strong artifacts at both side of Gaussian anomaly, which is introduced by the differential term in the objective function. The artifacts can be suppressed by the idea of image warping (Shen and Symes, 2013). Figure 3(b) shows the second term of gradient formula and figure 3(c) shows the cor-

rected gradient. Compared figure 3(a) and figure 3(c), we can see that the reflection effect is suppressed more after correction on the original one, which is coincident with the smooth assumption of background velocity in the linearized Born approximation .
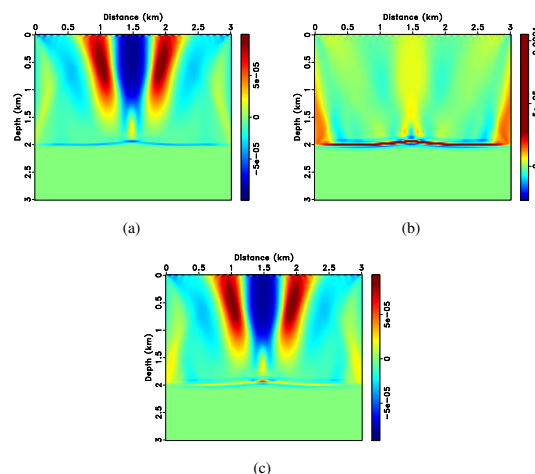

Figure 3: (a) The first term of gradient formula; (b) The second term of gradient formula; (c) The final gradient.

CONCLUSION AND DISCUSSION

Based on linearized Born approximation, we derive the gradient formula for both short scales and long scales of velocity model from the objective function which combines data fitting and differential semblance. The reflectivity is inverted with Chebyshev iteration in the inner loop of background velocity update and a corrected formula is also proposed in the background velocity gradient calculation. The numerical tests on Gaussian model show that: (1) the inverted reflectivity has higher resolution and more balanced amplitude; (2) compared with CG method, Chebyshev iteration method has a comparable convergent rate after estimating the spectrum bound of normal operator correctly; (3) the corrected gradient provides the update direction of background velocity and put more emphasis on transmission effect, which is coincident with linearized Born approximation.

However, there are still lots of work need to do. The first one is how to improve the efficiency of our proposed method, such as estimate spectrum bound quickly and accelerate convergent rate via preconditioning. Another more theoretical challenge is how to extend the idea to non-linear extended waveform inversion.

ACKNOWLEDGMENTS

EDITED REFERENCES
Note: This reference list is a copy-edited version of the reference list submitted by the author. Reference lists for the 2013 SEG Technical Program Expanded Abstracts have been copy edited so that references provided with the online metadata for each paper will achieve a high degree of linking to cited sources that appear on the Web.

REFERENCES

Almomin, A., and B. Biondi, 2012, Tomographic full waveform inversion: Practical and computationally feasible approach: 82nd Annual International Meeting, SEG, Expanded Abstracts, 1–5.

Biondi, B., and A. Almomin, 2012, Tomographic full waveform inversion (TFWI) by combining full waveform inversion with wave-equation migration velocity analysis: 82nd Annual International Meeting, SEG, Expanded Abstracts, 1–5.

Biondi, B., and P. Sava, 1999, Wave-equation migration velocity analysis: 69th Annual International Meeting, SEG, Expanded Abstracts, 1723–1726.

Biondi, B., and W. W. Symes, 2004, Angle-domain common-image gathers for migration velocity analysis by wavefield-continuation imaging: Geophysics, **69**, 1283–1298, http://dx.doi.org/10.1190/1.1801945.

Pratt, R. G., 1999, Seismic waveform inversion in the frequency domain, Part 1: Theory and verification in a physical scale model: Geophysics, **64**, 888–901, http://dx.doi.org/10.1190/1.1444597.

Rickett, J. E., and P. C. Sava, 2002, Offset and angle-domain common image-point gathers for shot-profile migration: Geophysics, **67**, 883–889, http://dx.doi.org/10.1190/1.1484531.

Shen, P., and W. Symes, 2013, Subsurface domain image warping by horizontal contraction and its application to wave-equation migration velocity analysis: Presented at the 83rd Annual International Meeting, SEG.

Shen, P., and W. W. Symes, 2008, Automatic velocity analysis via shot profile migration: Geophysics, **73**, no. 5, VE49–VE59, http://dx.doi.org/10.1190/1.2972021.

Stolk, C. C., M. V. de Hoop, and W. W. Symes, 2009, Kinematics of shot-geophone migration: Geophysics, **74**, no. 6, WCA19–WCA34, http://dx.doi.org/10.1190/1.3256285.

Sun, D., and W. W. Symes, 2012, Waveform inversion via nonlinear differential semblance optimization: 82nd Annual International Meeting, SEG, Expanded Abstracts, 1–7.

Symes, W., 2009, The seismic reflection inverse problem: Inverse Problems, **25**, no. 12, 123008, http://dx.doi.org/10.1088/0266-5611/25/12/123008.

Symes, W., and J. J. Carazzone, 1991, Velocity inversion by differential semblance optimization: Geophysics, **56**, 654–663, http://dx.doi.org/10.1190/1.1443082.

Symes, W. W., 2008, Migration velocity analysis and waveform inversion: Geophysical Prospecting, **56**, no. 6, 765–790, http://dx.doi.org/10.1111/j.1365-2478.2008.00698.x.

Symes, W. W., and M. Kern, 1994, Inversion of reflection seismograms by differential semblance analysis: Algorithm structure and synthetic examples 1: Geophysical Prospecting, **42**, no. 6, 565–614, http://dx.doi.org/10.1111/j.1365-2478.1994.tb00231.x.

Tarantola, A., 1984, Inversion of seismic reflection data in the acoustic approximation: Geophysics, **49**, 1259–1266, http://dx.doi.org/10.1190/1.1441754.

Virieux, J., and S. Operto, 2009, An overview of full-waveform inversion in exploration geophysics: Geophysics, **74**, no. 6, WCC1–WCC26, http://dx.doi.org/10.1190/1.3238367.